Geoderma 409 (2022) 115607

Contents lists available at ScienceDirect

Geoderma

journal homepage: www.elsevier.com/locate/geoderma

Earthworms, Darwin and prehistoric agriculture-Chernozem genesis reconsidered

Stefan Dreibrodt [a,b,*], Robert Hofmann [a,c], Marta Dal Corso [a,c], Hans-Rudolf Bork [a,b], Rainer Duttmann [a,d], Sarah Martini [c,e], Philipp Saggau [d], Lorenz Schwark [f], Liudmyla Shatilo [a,c], Michail Videiko [g], Marie-Josée Nadeau [h], Pieter Meiert Grootes [b,h], Wiebke Kirleis [a,c], Johannes Müller [a,c]

[a] CRC 1266 Scales of Transformation, Deutsche Forschungsgemeinschaft, Germany
[b] Institute for Ecosystem Research, University of Kiel, Germany
[c] Institute for Pre- and Protohistoric Archaeology, University of Kiel, Germany
[d] Institute of Geography, University of Kiel, Germany
[e] Department of Anthropology, Yale University, US
[f] Institute of Geoscience, University of Kiel, Germany
[g] Laboratory of Archaeology, Borys Grinchenko Kyiv University, Ukraine
[h] National Laboratory of Age Determination, Norwegian University of Science and Technology, Trondheim, Norway

ARTICLE INFO

Handling Editor: Karen Vancampenhout

Keywords:
Chernozem
Anecic earthworms
Soil Formation
Trypillia Chalcolithic Giant Settlement Sites
Anthropocene
Central Ukraine

ABSTRACT

Chernozems are among the most fertile agricultural soils on Earth and are important terrestrial carbon reservoirs. Since the Miocene-advent of grassland-ecosystems, they develop on fine-grained calcareous parent materials, generally in continental climates. So far, no theory explains all Chernozem occurrences. This limits modeling of their long-term soil carbon dynamics. Insights gained on Chernozems that buried prehistoric archaeological features in central Ukraine provide a key. Prehistoric agriculture favored anecic earthworm abundance and anecic earthworm surface casting delivers the best explanation for coeval Chernozem genesis, its properties, and distribution, an idea originally put forward by Darwin. Anecic earthworms transfer soil material upwards due to the necessity to clear their vertical burrow permanently from material fallen in. While Chernozems in the climatic steppe form under climate conditions that limit epigeic and endogeic earthworms naturally, the patchy and time-transgressive Chernozem occurrences in temperate humid Europe would reflect sites where the proliferation of anecic earthworms at the expense of the former ecological groups resulted from early Anthropocene landscape transformations. We will have to add anecic earthworms to the Neolithic Package that identifies the socio-economical transformations related to sedentarism and evolving agrarian production modes of cereal cultivation and animal husbandry.

1. Introduction

Chernozems (Mollisols, "Black Earth") cover approximately 230 million hectares of the Earth's land surface (c. 7 %) over zones with dry continental climate on calcareous Loess (e.g. Driessen et al., 2001; FAO, 2014). In general, Chernozem profiles are composed by a thick organic rich surface horizon above the parent material. Although studied since a long time (Dokuchaev, 1883), there is no consensus about the formation and genesis that would explain all Chernozem occurrences. The unusually thick organic accumulation has been attributed to continental steppe climate conditions, limiting organic matter decomposition (Dokuchaev, 1883). Yet, Chernozems occur also in European temperate humid climates (Soil Atlas of Europe, 2015; Eckmeier et al., 2007) (Fig. 1a) and tropical grasslands of Africa (e.g. Eswaran et al. 1997) or India (e.g. Singh and Ram, 1996). Thus, the initial idea of zonal soil formation has been challenged. The frequent abundance of burrowing mammals has been considered a factor in Chernozem formation, but their activity does not explain soil homogeneity and "linear soil organic matter (SOM) age-depth gradients" (Scharpenseel et al., 1986). Occurrences in temperate humid Europe have been considered to reflect early

* Corresponding author at: Institute for Ecosystem Research, University of Kiel, Ohlshausenstraße 40, 24098 Kiel, Germany.
E-mail address: sdreibrodt@ecology.uni-kiel.de (S. Dreibrodt).

https://doi.org/10.1016/j.geoderma.2021.115607
Received 25 June 2021; Received in revised form 22 October 2021; Accepted 18 November 2021
Available online 25 November 2021

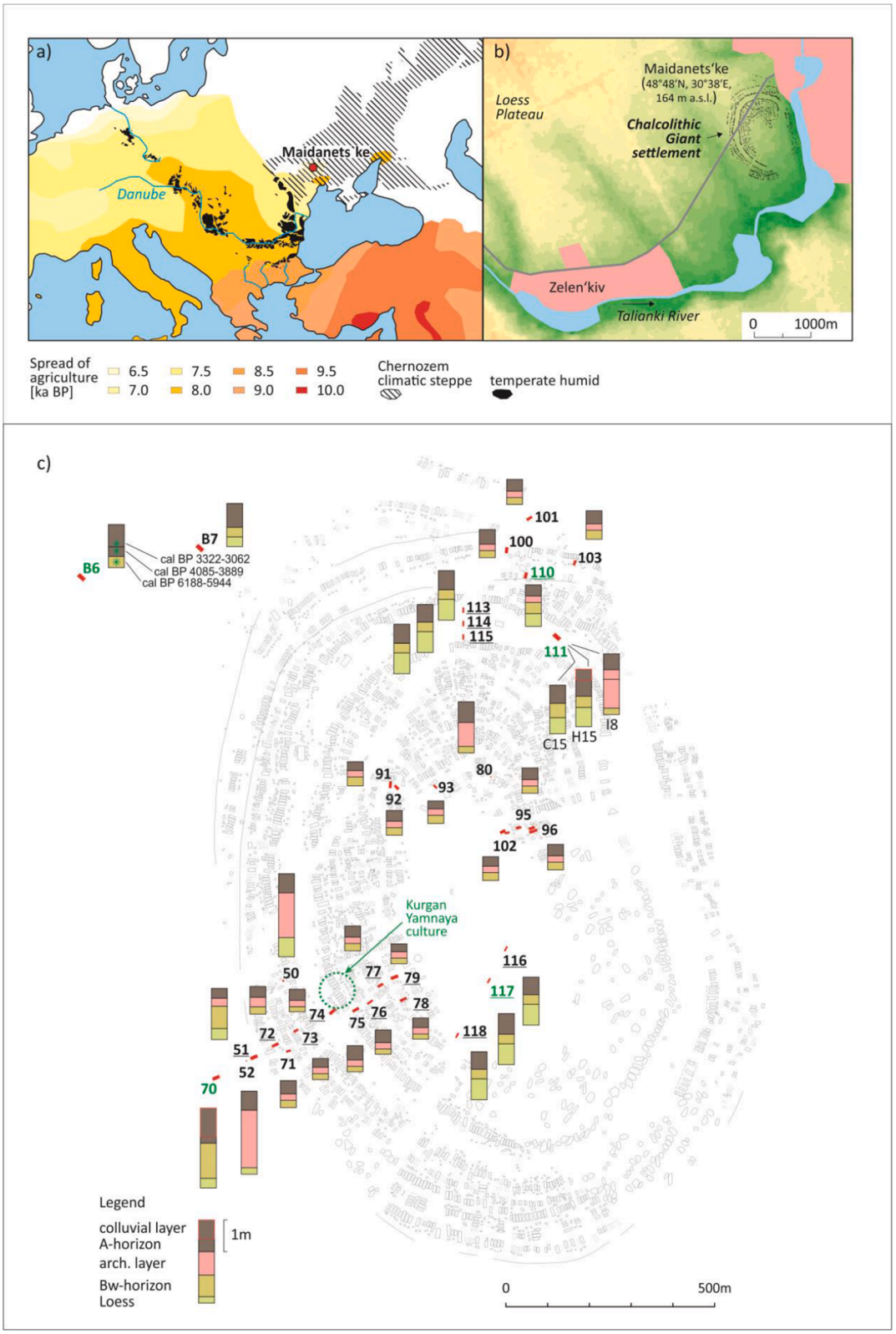

Fig. 1. a) Distribution of Chernozem in Europe (Eckmeier et al., 2007, Soil Atlas of Europe, 2005, Tanov, 1956); temperate humid Chernozems follow the track of the European Neolithic transition (Vander Linden and Silva, 2018, Bánffy et al., 2019), rivers and their valleys being considered as migration vectors, b) Location of the Chalcolithic Giant settlement Maidanets'ke on a Loess plateau, c) magnetic map indicating the position of burned house remains, location of the sampled profiles (red) and their pedo-stratigraphy (columns) within the giant Chalcolithic settlement; green numbers- radiocarbon dates, underlined- laboratory analyses; radiocarbon ages (bulk SOM) of offsite profile B6, 2δ probabilities. (For interpretation of the references to color in this figure legend, the reader is referred to the web version of this article.)

Holocene relict soils (e.g. Kabała et al., 2019); however, radiocarbon ages and palaeoecological studies (e.g. Eckmeier et al., 2007) challenge the early Holocene interpretation of all temperate humid Chernozems. Black carbon (BC) in temperate humid Chernozems led to the idea of fire-related Chernozem formation (e.g. Schmidt et al., 2002), partly attributed to early farmers (Gehrt et al., 2002). Yet, ambiguous BC-radiocarbon ages and the lack of a process explaining the thick organic horizon resulted in a failure to explain Chernozem genesis.

The present study, carried out on Chernozems in central Ukraine, delivers results that enhance insights into timing and processes of Chernozem genesis, allowing putting the partly contradicting results from the literature into a coherent picture, and thus provides a new base to understand Chernozem genesis in general.

2. Regional setting

The giant Chalcolithic Trypillia C1 archaeological site at Maidanets'ke is situated in the forest-steppe ecotone of central Ukraine (Müller et al., 2017), district of Talne (Fig. 1). Archaeological sites of this type are unique because of their extremely large dimensions. At Maidanets'ke, on an area of 200 ha approximately 3000 houses arranged in a series of oval structures around an unbuilt central space were inhabited approximately from 3990 to 3640 BCE (e.g. Müller et al., 2017; Ohlrau, 2020; Pickartz et al., 2019). Surveys of the many potshards present on the recent surface, magnetic surveys, excavations and exhaustive dating campaigns revealed that about 1500 houses were inhabited contemporaneously by probably > 10,000 people (Ohlrau, 2020; Pickartz et al., 2019). The archaeological record of these settlements comprises of burned house remains, pits with a varying depths and fillings, pottery kilns, and, rather seldom, un-burned house remains. The remnants of a burned house are usually characterized by a floor layer containing a varying amount of earthen artefacts (pottery, vessels etc.), that is covered by a layer of burned remains of the house walls (daub). The daub layer is the main (mass, volume) component, varying in thickness (5–30 cm), extension (c. 4 × 10 m to 7 × 15 m) and density as a result of the given architecture, inhabitation and the individual burning process of the house.

The climate in the region is humid continental (Dfb) today, with hot summers and cold wet winters (www.climate-data.org, 2020). The potential natural vegetation of the region belongs to the climate sensitive forest-steppe transition zone. The investigated site is situated on a Loess plateau grading towards the valley of the adjacent Talianky River (Fig. 1b). The Loess plateau is used for large agricultural fields, meadows and shrubs as well as ponds cover parts of the valley nowadays. Where there is no agricultural land use, deciduous forests are recovering the landscape today. The surface soils are classified as particularly thick Chernozems in the research area (Atlas of Soils of the Ukrainian SSR, 1979; Machow, 1929). Extensive archaeological work revealed that the Chernozem covers settlements of the Chalcolithic Tripyllia C1 phase in the region (Müller et al., 2016; 2017; Kruts, 2012; Chapman et al., 2016). No Chernozems are present below the Tripyllian settlements in the steppe-forest ecotone of central Ukraine. Instead incipient Bw horizons are preserved in varying thicknesses. Humus horizons of a thickness of 10–15 cm were recorded during excavations of burial mounds ("Kurgan") of the Yamnaya culture (c. 5,050–4,450 cal BP) at Maidanets'ke (Fig. 1c) and other sites of the region (Shmaglij and Videiko, 1988; Ivanova, 2016). Since we argue, that these humus horizons later developed into the present Chernozems by further growth in thickness, we call it "incipient-Chernozems" in the following. A reconstruction of Holocene soil erosion at slopes adjacent to the giant settlement of Maidanets'ke revealed phases of slope instability that coincide with global (cal 27.6 +/- 1.3 kyrs BP, 12.0 +/- 0.4 kyrs BP), northern hemispheric (cal 8.5 +/- 0.3 kyrs BP), Mediterranean (cal 3.93 +/- 0.1 kyrs BP) as well as western to central European (2700 to 2000 cal BP) climate anomalies (Dreibrodt et al., 2020). Prehistoric land use was not reflected by slope instability in the sediment record.

3. Materials and methods

3.1. Field methods

34 soil profiles were studied with field methods (Fig. 1c). The presence and thickness of diagnostic horizons (FAO, 2014) and archaeological remnants was documented using standard protocols (AG Boden, 2005), scaled sketches and digital photography. From 23 profiles (16 above burned houses, 1 above a pit fill, 6 on unbuilt space) samples for laboratory analysis were taken in continuous depth increments (from 5 cm to 15 cm). From four profiles, samples for bulk density determination were taken in steel cylinders (100 cm^3, 3 replicates). Additionally, loose earthworm casts that cover the soil surfaces in profiles along tree lines planted in 1974 in between the agricultural fields were sampled for standard laboratory analysis (Fig. 2a). The position of the profiles selected for field and laboratory analysis is displayed in Fig. 1c.

3.2. Laboratory methods

3.2.1. Geophysical and geochemical analysis

Laboratory analysis was carried out on the air dried < 2 mm fraction. Sample pre-treatment included a careful disintegration of the dry samples (room temperature) with the help of mortar and pestle, and sieving through a 2 mm mesh. During this step, all visible artefacts, bio-remains, and stones were extracted carefully and weighed separately. Special care was taken to remove all visible particles from the samples, which originate from the underlying archaeological features. The following laboratory analysis was restricted to the < 2 mm fraction. The RGB-colours of the samples were determined in three replicates on a Voltcraft Plus RGB-2000 Colour Analyser set to display in a 10-bit RGB colour space (e.g. Rabenhorst et al. 2014; Sanmartín et al., 2014). Since RGB colours are internally highly correlated, these data were converted into Light Intensity, Hue, and Colour Saturation according to Viscara Rossel et al. (2006). The volume specific magnetic susceptibility was measured on three replicates of weighed 10 ml- samples using a Bartington MS2B susceptibility meter (resolution $2*10^{-6}$SI, measuring range 1–$9999*10^{-5}$SI, systematic error 10%). Measurements were carried out at low (0.465 kHz) and high (4.65 kHz) frequency. A 1% Fe_3O_4 (magnetite) sample was measured regularly and the samples susceptibility values were calibrated using this standard before the mass specific susceptibility values were calculated. Mass specific magnetic susceptibility and frequency dependent magnetic susceptibility (FD) were calculated according to Dearing et al. (1996). Soil organic matter (SOM) and carbonate contents were estimated by Loss on Ignition (LOI) at 550 °C and 940 °C after two hours heating of formerly dried samples (105 °C overnight). On 15 profiles, the total carbon (TC), total nitrogen (TN) and total inorganic carbon (TIC) contents were measured with a Heraeus elemental analyser and converted into total organic carbon (TOC), soil organic carbon (SOC) and $CaCO_3$ values. The total elemental contents of the samples were measured on a p-ed-xrf device (NITON XL3t 900-series) of Thermo Scientific Analysers. For p-ed-xrf measurements, first, the < 2 mm fraction was ground in an Agate mill and placed in a plastic tube covered by a 4 μm thick film. These were then measured in a lead-mantled measurement chamber with He-flotation using the "mining, Cu/Zn" settings for 300 s with the p-ed-xrf device. As the device has the ability to not just record quantitative elemental concentrations, but also reports measurement errors, all elements with > 10 % error were discarded from further analysis. The adjustment of the measurement conditions were carried out according to instructions given in previous papers (Lubos et al., 2016; Martini et al., 2019), that included a calibration of the p-ed-xrf measurements on a wd-xrf data set (Dreibrodt et al., 2017). For selected profiles, the grain size distribution of the < 2 mm fraction was determined using a combined wet sieving (sand) and Atterberg (silt, clay) method. For profile 117 ground powder samples were analysed with the conventional xrd method (Siemens diffractometer, Cu-α radiation, 2 Theta 4–90°, step size 0.02, 1 s per step).

Fig. 2. Photographs of selected profiles: a) Profile 117, loose earthworm surface casts layer (3–4 cm) between agricultural fields, accumulated 1974–2016, b) Profile 77 illustrates a typical pedostratigraphy of the site, c) Profile 70 shows the incipient-Chernozem buried by colluvial layers and the thick preserved relict Bw horizon; note the deep disturbance by burrowing mammals and carbonate filled abandoned earthworm and root channels.

Identification of present mineral assemblages was carried out using d-spacings given in soil mineralogy textbooks (e.g. Brindley and Brown, 1980). At profile 117, investigations were supplemented with organic geochemistry. Organic isotope analysis was performed on the decalcified (10%HCl) sample material using a Thermo Finnigan Delta V irMS coupled to a Flash EA via a ConFlo III interface following standard procedures. Isotope values are reported relative to the Vienna Pee Dee Belemnite standard (V-PDB). Lipids were extracted using pressurized liquid Extraction (DIONEX ASE200) using a solvent mixture of hexane/dichloromethane (9/1; v/v) and separated into non-polar and polar compound classes by automated SPE (LC-Tech Freestyle) on 2 g of pre-extracted and activated silica. Non-polar compounds were eluted with hexane/dichloromethane (9/1; v/v) and subjected to gas chromatography-mass spectrometry (GC–MS) using an Agilent 7890A GC equipped with a Phenomenex Zebron ZB-5 column (30 m × 0.25 mm i.d.; 0.25 μm film thickness) and coupled to an Agilent 5975B mass chromatograph. The injection temperature was held at 60 °C for 4 min, after which the oven temperature was raised to 140 °C by 10 °C/min and subsequently to 320 °C by 3 °C/min, at which it was held for 8 min. The MS was operated at an electron energy of 70 eV and an ion source temperature of 250 °C. The homologues series of n-alkanes was detected via the $m/z = 85$ mass chromatograms and peak areas used for calculation of relative abundance ratios.

For a PCA of the Chernozem Ah horizon, 19 parameters were selected. Those comprise of colour values (Hue, Light Intensity, Chromatic Information), LOI 550/ 940, magnetic susceptibility (low frequency, mass specific), frequency dependent magnetic susceptibility, and p-ed-xrf-total elemental contents (P, Zr, Y, Sr, Rb, Zn, Fe, Ti, Ca, K, Al, Si). All percentage values were logarithmised prior to the application of PCA analysis (e.g. Filzmoser et al., 2009).

3.2.2. Radiocarbon dating

Forty samples of five profiles were selected for radiocarbon dating of SOM. Radiocarbon dating of bulk organic soil samples was performed both at the Poznan Radiocarbon Laboratory and at Beta Analytics. The samples were extracted with HCl to remove carbonates. The subsequent removal of the acid also removed the acid soluble fulvic acids, leaving a mixture of humic and humin substances to be dated. A more extensive sample extraction was carried out at the National Laboratory for Age Determination in Trondheim, Norway. The samples were treated according to Seiler et al. (2019). They were demineralised with 1 % HCl and concentrated acid was added until the pH was stable at 1 for at least one hour. The samples were then washed with deionized water to pH > 4. The samples were then treated with 1% NaOH to remove the alkali soluble humic acids (HA). The solution was separated from the solid fraction by centrifugation and decantation. The humic acids were precipitated from the solution by acidifying with concentrated HCl to pH 1 and then washed with deionized water to pH > 3. The solid humin fraction (AR) was washed with de-ionized water to pH < 10 and acidified to pH 1 using concentrated HCl before being washed a last time to pH > 3. During these steps, we allocated sufficient time for the liquids to penetrate the fine sediment and made sure that the pH was stable before proceeding to the next step. All the solutions and wash waters were kept for measurement of the ^{14}C concentration of their organic content at a later time. The radiocarbon content of the AR and HA fractions presented in this article was measured according to Seiler et al. (2019). Radiocarbon ages were calibrated using the IntCal13 data set (Reimer et al., 2013). Age depth models of the profiles dated in continuous depth increments were constructed using the oxcal software (Bronk Ramsey and Lee, 2013).

4. Results

4.1. Composition of the Chernozem

4.1.1. Pedostratigraphy

The pedostratigraphy at Maidanets'ke is comprised by calcareous Loess (10YR7/2–3), a relict Bw horizon (10YR6/4–6), and the (Chernozem) Ah horizon (10YR4/2–3-10YR3/2–3). The archaeological record (burned house remains) is situated on top of the rBw and buried by the Ah horizon. The daub layers show often a dip towards its outer parts, where it is buried deeper by the surface Chernozem than in the center of thick archaeological layers. Filled animal burrows (krotovina) and perpendicular fillings of root and earthworm channels, often containing secondary carbonate concretions, penetrate the whole sequence.

The thickness of the relict Bw-horizon and the Ah horizon varies in

the investigated profiles. The Ah horizon has a significantly smaller thickness over remnants of burned houses compared to profiles over pit fills or unbuilt space . The rBw is thicker in profiles that became buried by subsequent colluviual layers (profile 70, Fig. 1c, 2c, 7a) or covered by a thick archaeological layer (profile 52, Fig. 1c). Below a burial mound of the Yamnaya culture (Fig. 1c) a "incipient-Chernozem" has been recorded (Shmaglij and Videiko, 1988). Similarly, in trench 70 a "incipient-Chernozem" was found buried by a sequence of younger colluvial layers.

An important field observation was made in between the nowadays intensively used agricultural fields. In the shelter of tree lines planted in 1974, a layer of loose earthworm aggregates has been accumulated until 2016 atop unplowed soil (Fig. 2a). Systematic measurements in trench 117 resulted in a mean thickness of 3–4 cm of this accumulation.

4.1.2. *Geophysical and geochemical properties*

Fig. 3 gives results of geophysical and mineralogical analyses of selected profiles. Fig. 3a shows the grain size distribution of three profiles. In general, the profiles are characterized by a silty (coarse, middle) to clayey grain size. The Ah horizons are characterized by higher contents in fine particles, most pronounced in profile 117. In c. 80–100 cm, a slight increase in sand is displayed, again most pronounced in profile 117. The bulk density values are displayed in Fig. 3b. There, with some variation, the majority of samples have values between 1.2 and 1.4 g*cm^{-3}. The higher values in lower depths are probably related to recent plowing layers. Fig. 3c shows the mineral assemblage of the soils at the site. It consists of quartz, feldspars, and clay minerals (illite, expandable clays/ chlorite, kaolinite) and calcite. The Loess contains more calcite than the Chernozem. There is no indication for a substantial addition of material to the Chernozem different from the Loess.

The distribution of lipid biomarkers from profile 117 is displayed in Fig. 4. A mixture of lipids of tree and grass origin, dominated by the former, characterizes the Ah horizon. A calibration with present day samples from the research area indicate ash (*Fraxinus*) leaves as a main component of the tree lipids. The transition of Ah to the rBw shows a similar pattern of dominant tree lipids within the sample. Contrastingly, the organic carbon fraction within the calcareous Loess samples is dominated by lipids of grass plant origin.

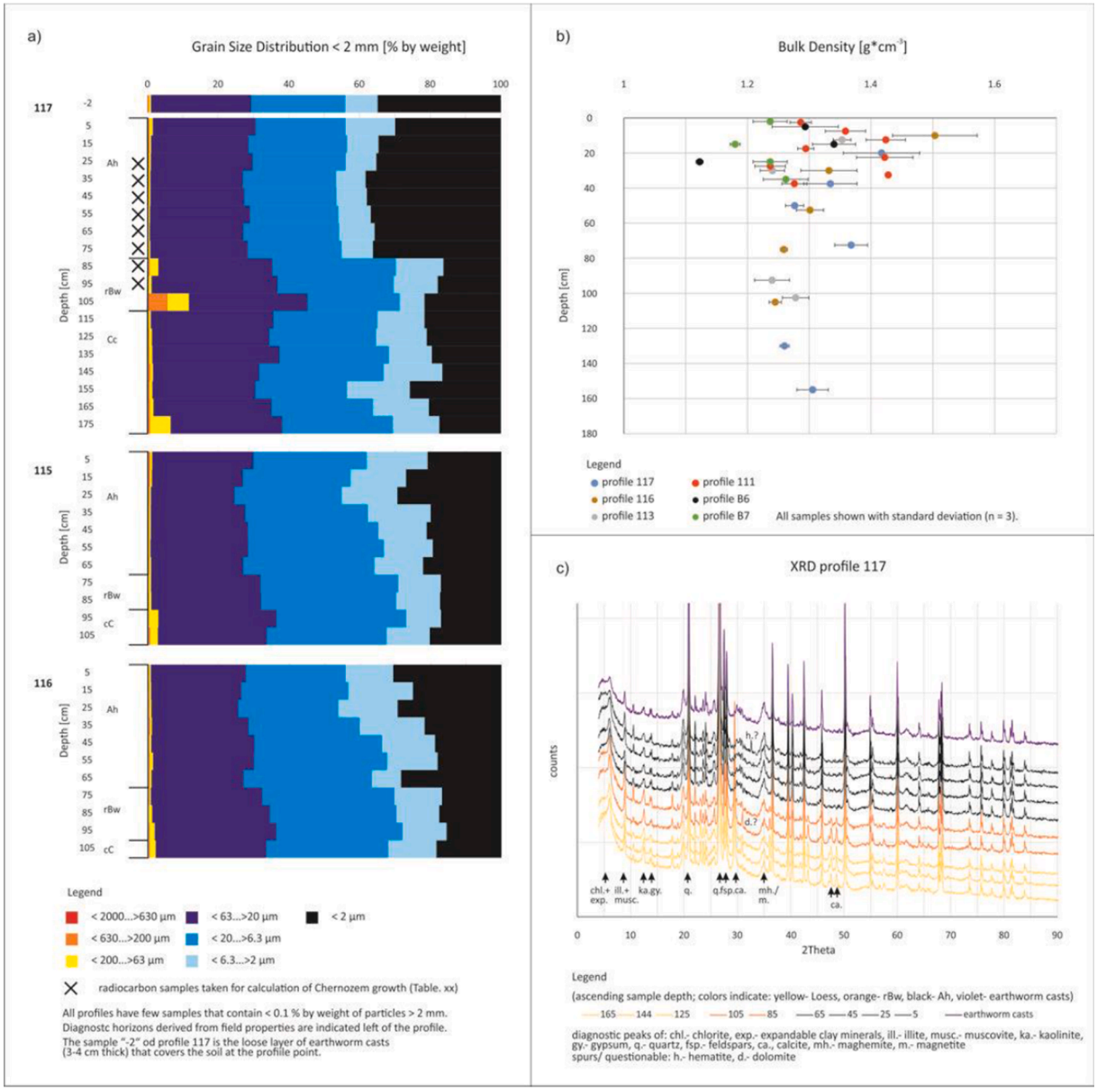

Fig. 3. Geophysical and mineralogical results of selected profiles. a) Grain size distribution, b) bulk density, c) xrd mineral assemblage of profile 117.

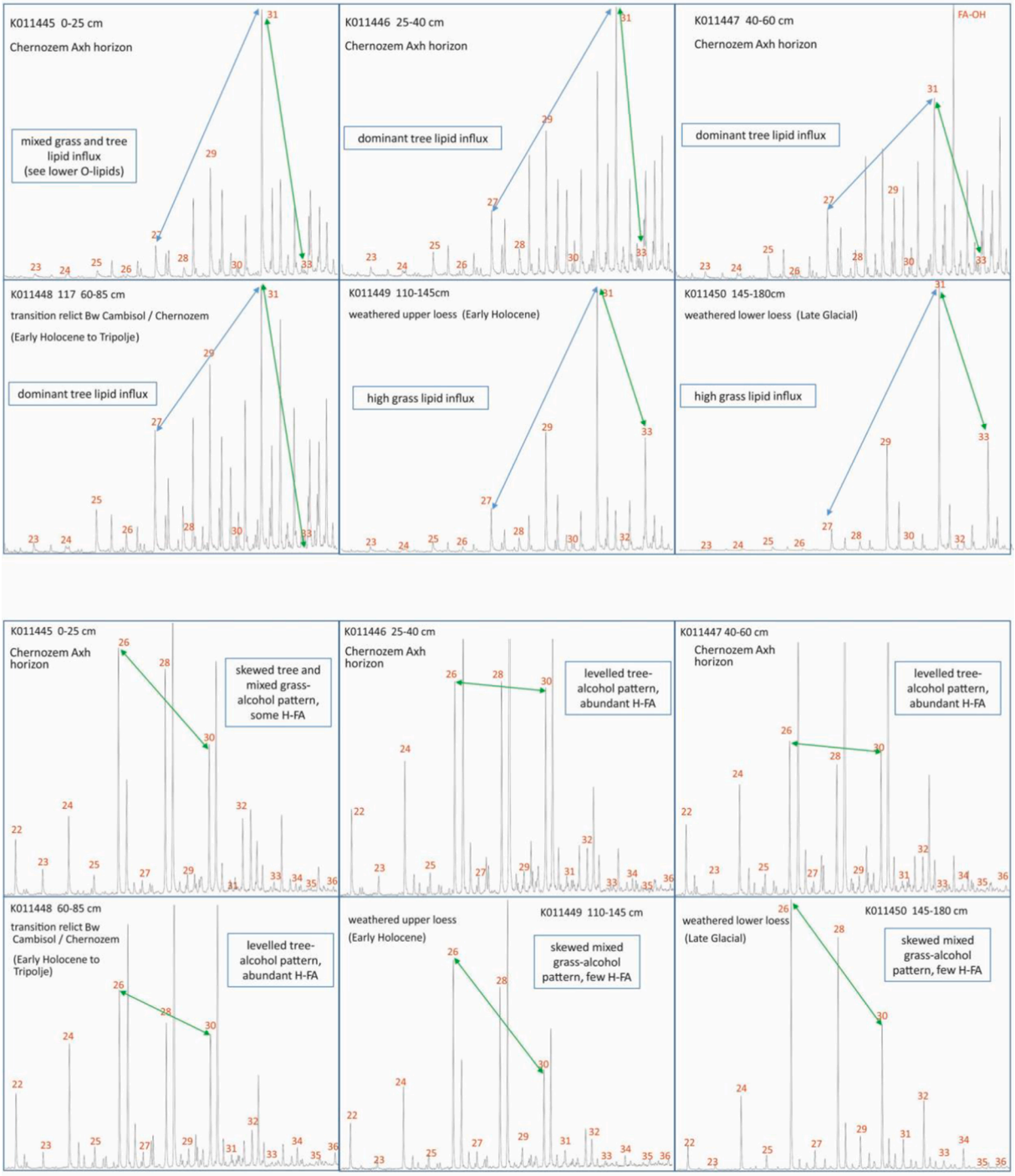

Fig. 4. Distribution of lipid biomarkers derived from either predominantly grasses or trees (upper block: distribution of n-alkanes, lower block: distribution of n-alcohols). Grass lipids dominate in samples taken in 100 to 180 cm depth, as seen from the high proportion of nC_{33} alkanes and low relative contribution by n-alcohols. Dominantly tree-derived lipids prevail between 25 and 85 cm depth, as indicated by levelled distribution of *n*-alcohols and low proportion of nC_{33} alkane. A mixed grass/tree influx is noted for the top soil layer by elevated C_{26}-alcohol but low abundance of nC_{33} alkane.

Fig. 5 Fig. 6 gives additional data of complete profiles. Fig. 5a shows the deep profile 117 as an example for a section in unbuilt space. The TOC values are the highest in the surface samples of the Ah, grading stepwise to lower values at the base of the Ah. From the rBw towards the cC a further stepwise decrease is displayed exposing the lowest TOC values in the Loess. While the Ah contains very few TIC, a stepwise increase is visible in the rBw towards the cC. The Loess shows the highest TIC values in its upper part. The total organic carbon: nitrogen ratio decreases from the Ah towards the Loess. RGB colors indicate darkest colors of the Ah horizon, a transition to more dark brownish colors in the rBw and pale brownish values in the cC (Loess). The magnetic properties of the profile show slightly higher FD values in the Ah, and a weak trend to lower FD values in the rBw and the Loess (in particular its upper part). Mass-specific susceptibility show the highest values in the upper 30 cm of the Ah, followed by a trend towards lower values through the Ah and the rBw, cumulating in minimum values within the cC (Loess). Total phosphorus contents is highest in the Ah horizon and characterized by decreasing values in the rBw and in particular at the base of the Loess.

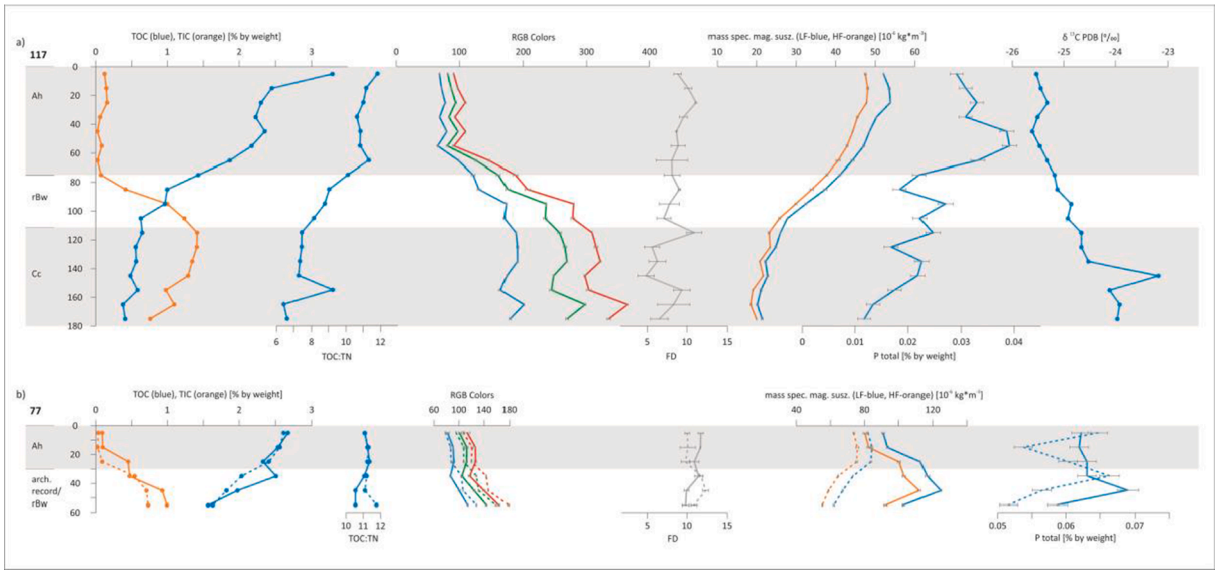

Fig. 5. Selected results of laboratory analysis on a) the long undisturbed profile 117 in unbuilt space and b) profile 77 trough/ beside a burned house (continuous/ dashed line).

The highest values in phosphorus are present in the lower part of the Ah horizon. The δ ^{13}C values show an almost linear trend of lighter values with depth, except of one value in the Loess (perhaps disturbed by an overseen krotovina). As an example for a sequence cutting through the archaeological record, laboratory results from exposure 77 are displayed in Fig. 5b. The continuous lines show data of the profile including the archaeological layer. The dashed lines show data c. 50 cm aside from the archaeological record. The TOC, TIC, TOC:TN, and RGB color values and trends resemble the data observed in the unbuilt profile 117. Remarkable differences to the unbuilt space profile 117 are visible in the magnetic properties and the total P contents. The values of FD, mass-specific susceptibility as well as total P are significantly higher in the Chernozem of profile 77 compared to profile 117, in particular directly above the archaeological remains.

A comparison of the mean values from all analyzed Ah horizons (Fig. 6) displays the significance of the different properties between Chernozem above archaeological record and unbuilt space. (The complete data set of the Ah horizons is given in supplemental Table 1.) While LOI and RGB colors do not differ, Ah horizon thickness, magnetic properties and total phosphorous content differ significantly. Additionally, a mean value comparison of the TOC, TIC and TOC:TN ratio carried out for Chernozem profiles above houses and unbuilt space indicates significant differences of the organic matter in the soil above the archaeological record compared to profiles on unbuilt space (TOC values, TOC:TN ratios).

4.2. Radiocarbon ages and age depth-profiles

Fig. 7 shows oxcal plots of four Chernozem profiles in high resolution. Measurements of different fractions of SOC are indicated by color. The inhabitation interval of the giant Chalcolithic settlement, inferred from 67 radiocarbon dates from the archaeological contexts (Ohlrau, 2020), is indicated.

In profile 70, situated at a slope beneath the prehistoric settlement, a buried "incipient-Chernozem" was found at c. 85 to 105 cm depth. It is underlain by a Bw horizon, that contains remnants of early Holocene organic carbon. The observed gap between the two lowermost radiocarbon ages is probably reflecting an erosional hiatus, since intensive erosion occurred at c. 8000 cal BP at the site (Dreibrodt et al., 2020). The radiocarbon ages of all measured fractions at its base indicate a start of the "incipient-Chernozem" formation during the inhabitation of the giant Chalcolithic settlement. In the upper part of the "incipient-Chernozem" the age difference between HA and AR becomes larger, demonstrating the age inhomogeneity of SOM. The soil became covered by a first colluvial layer at c. 4000 cal BP, according to the radiocarbon age of the soil organic matter of the colluvium and an embedded large Bronze Age pottery shard (Kirleis and Dreibrodt, 2017; Dreibrodt et al., 2020). Subsequent erosion at c. 2500 cal BP and later on resulted in the accumulation of 85 cm colluvium that covers the "incipient-Chernozem" today.

In profile 117, situated at a plateau situation of the unbuilt center of the settlement, the HA and AR ages of the relict Bw horizon show a more continuous transition from early Holocene into to the occupation period of the giant Chalcolithic settlement. In the lower part of the rBw, HA and AR ages are similar. At the base of the Chernozem Ah horizon, the difference between HA and AR ages becomes larger. The HA age is in accordance with an onset of Chernozem formation during the inhabitation time of the giant Chalcolithic settlement, while the AR ages are too young. Towards the recent surface the age-depth gradient becomes steeper and the difference between HA and AR ages becomes smaller.

Profiles 110 and 111 cut through the archaeological record. Profile 110 contains a thin, broken-up daub layer of a dated burned house at the base of the Ah horizon at 37 cm. The organic matter of the complete sequence is younger than the archaeological record. AR and HA ages are very similar in the upper part and near the bottom of the profile. The AR ages increase below the daub layer while the mobile HA ages vary and are younger down to ~ 60 cm. In profile 111, the Ah horizon covers a thick stack of archaeological layers, comprising a levelling layer, topped by a floor and daub layer. The AR ages of the rBw horizon transition from the early Holocene to the occupation phase of the giant Chalcolithic settlement. The organic matter of the Ah horizon of the surface Chernozem above the daub layer dates too young by c. 2000 to 3000 years compared to the archaeological record, both in AR and HA.

Bulk soil organic matter radiocarbon dates from an offsite profile (B6, Fig. 1c) indicate the last substantial addition of organic carbon to the rBw some decades before the foundation of the giant Chaloclithic settlement (cal BP 6188–5944).

Summarizing: In deeper and sheltered parts of the profiles, the radiocarbon ages are in accordance with an onset of Chernozem formation during the inhabitation time of the giant Chalcolithic settlement site. This is the case for the Chernozem and the buried forest soil in profile 70 under colluvial layers and in the deeper part of the

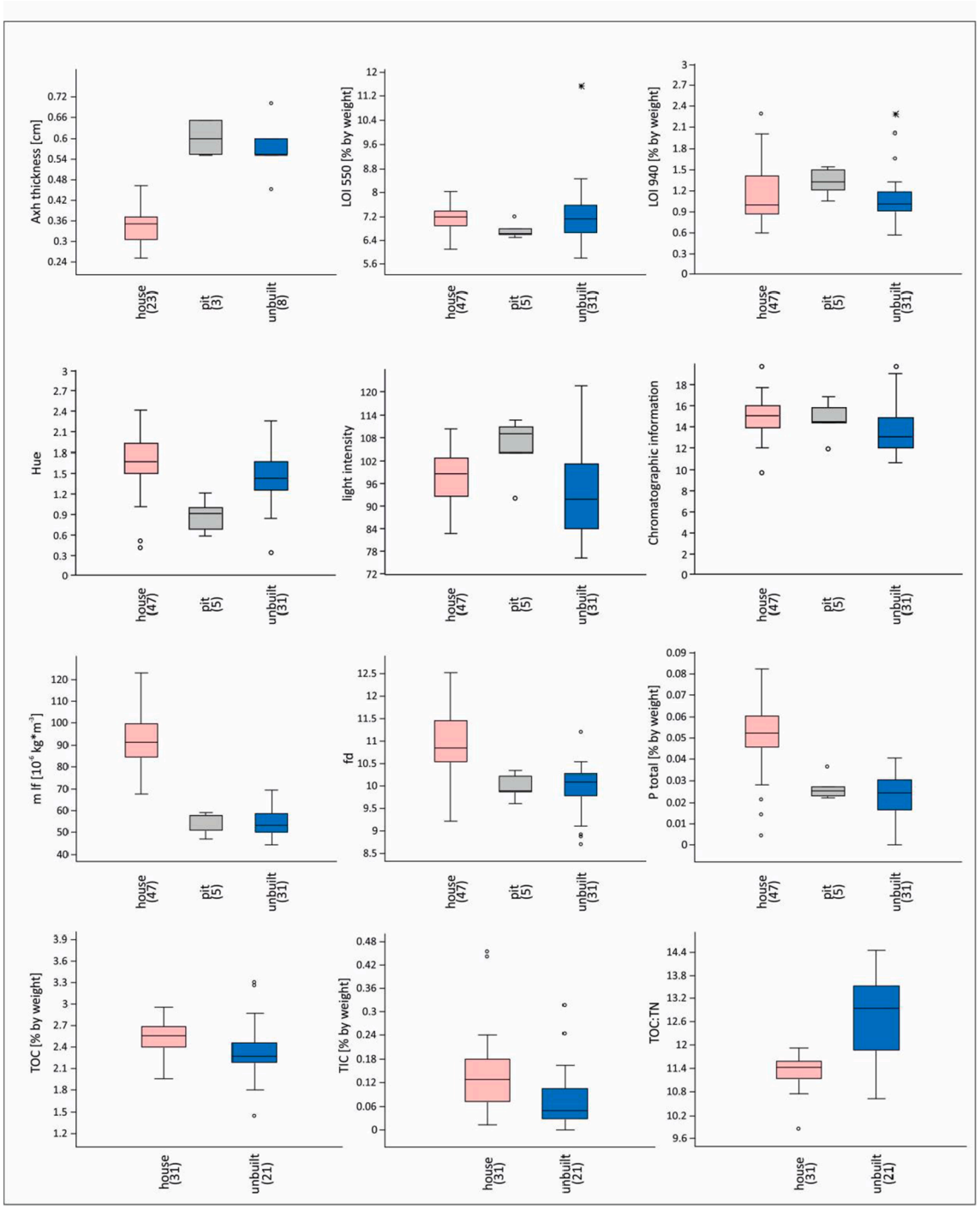

Fig. 6. Boxplots of laboratory data Ah horizons- Comparison of means; Chernozem above: burned houses (red), a pit fill (grey), unbuilt space (blue), number of samples in brackets. (For interpretation of the references to color in this figure legend, the reader is referred to the web version of this article.)

undisturbed profile 117. Below the daub and thick archaeological deposition in profile 111 and in the offsite profile B7 the SOM radiocarbon ages indicate the last significant input of organic matter into to relict forest soil shortly before the foundation of the giant prehistoric settlement site. Contrastingly, the thin Chernozem above archaeological layers displays "too young radiocarbon ages". Difference in the ages of HA and AR of the samples indicate SOM heterogeneity and different processes of organic matter turnover in different profile depths.

5. Discussion

5.1. Chernozem formation at Maidanets'ke, central Ukraine

While in the natural, climatic steppe, smaller Trypillia sites occur on top of Chernozems (Matviishyna and Doroshkevych, 2016), in the forest-steppe ecotone of Ukraine, Trypillia giant sites are buried by Chernozem (Müller et al., 2016, 2017; Kruts, 2012; Chapman et al., 2016) (Fig. 2b). The study of 35 trenches revealed a brownish relict forest soil horizon (rBw) beneath Maidanets'ke. Radiocarbon ages from the rBw horizon imply a last substantial addition of organic carbon to

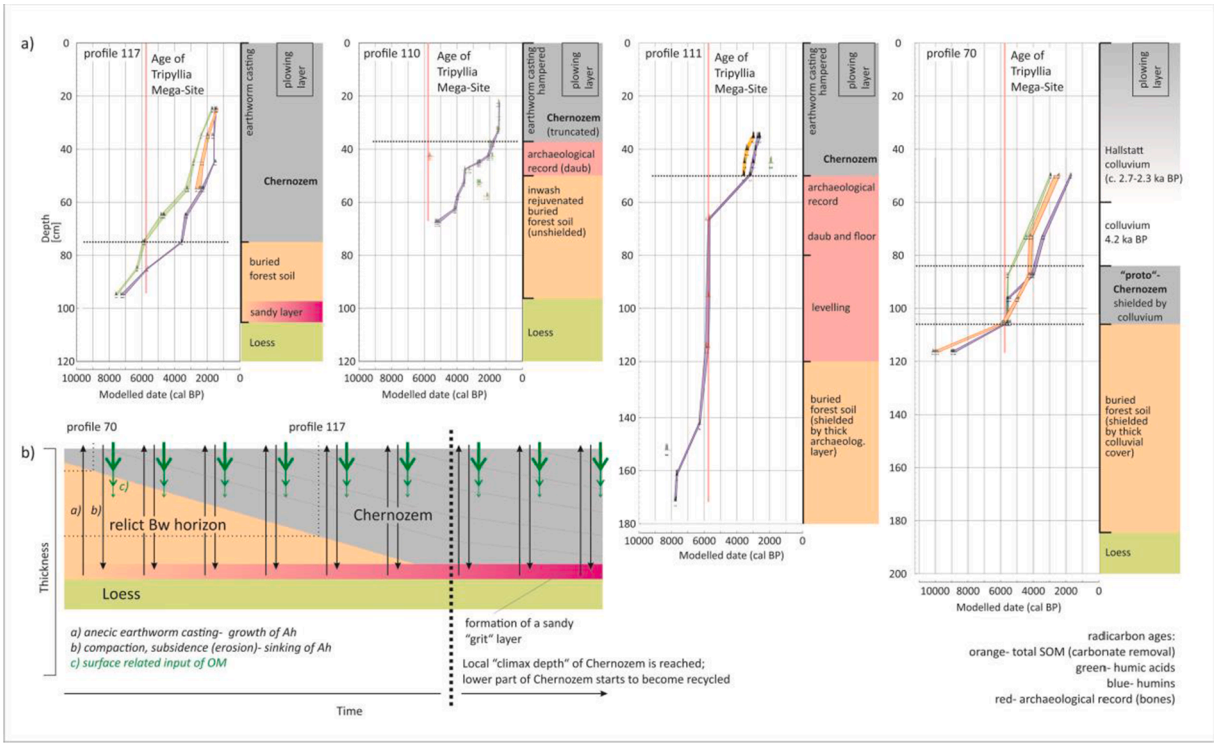

Fig. 7. ^{14}C apparent age vs. depth of four profiles and conceptual model of Chernozem genesis. a) Below the colluvial cover of profile 70, the daub floor of profile 111 and at the base of the thick Chernozem in Profile 117 the SOM is protected against contamination by young carbon and ages indicate Trypillyan activity. The long undisturbed profile 117 shows a radiocarbon age profile where the Chernozem-cast layer thickness has not yet reached the local earthworm digging depth (c. 100 cm). Old SOM from the evolving Chernozem becomes included in the casts and counteracts the effect of the incorporation of younger material from the surface. A "grit layer" starts to form at the profile base. Unshielded 'ages' above the archaeological horizon reflect hampered casting and the input of fresh photosynthate from the surface. Note that the summed thickness of relict B horizon and Chernozem remains similar. b) model of Chernozem genesis by anecic earthworm casting. After the start of the anecic surface casting process the Chernozem is growing at the same rate as it is sinking. When the Chernozem thickness equals the local mean burrowing depth, no further thickness growth is observed. Instead, the lower part of the Ah horizon starts to become involved in the casting process.

this soil horizon shortly before the foundation of the giant Chalcolithic settlement site. SOM radiocarbon ages at the base of undisturbed Chernozems and of buried "incipient-Chernozem" horizons indicate the start of Chernozem formation coeval with the foundation of Trypillian giant settlements.

The unique population agglomeration in the Ukrainian forest-steppe-ecotone followed a crisis of Chalcolithic societies in South-Eastern Europe (Harper, 2019) and could reflect a large-scale migration of people. This is indicated by the layout of Trypillia giant settlements (Fig. 1c) that implies a planning process (Ohlrau, 2020). Regional paleoclimate records (Kremenetski, 1995; Gerasimenko, 1997; Novenko et al., 2016) indicate no pronounced enduring climate shift between 6,000 and 4,500 cal BP. A dry phase recognized at c. 6,000 cal BP (Gerasimenko, 1997) coincides with other northern hemispheric climate records (e.g. Mayewski et al., 1997; De Menocal et al., 2000; Bond et al., 2001; Weninger et al., 2009) but is too short and weak to have had an enduring effect on the Eurasian steppe border biome. However, it might well have caused the crisis of the Cucuteni settlements and triggered the migration of people towards the Ukrainian forest-steppe border. The Trypillia subsistence system provided a maximal population size of c. 10,000 people inhabiting c. 1,500 houses at Maidanets'ke between c. 5,750–5,650 cal BP (Müller et al., 2017; Hofmann et al., 2019) with crops, domestic livestock, fuel, and game (Dal Corso et al., 2019). For the subsistence of this large population, substantial impacts on the given forest steppe ecotone were necessary. The houses constructed in a wattle and daub technique, and the everyday life (cooking fire, heating), both resulted in an immense need of wood and consequently a large deforestation. Additionally, areas for food production (cereals, cattle) to supply c. 10,000 people were created. The resulting prehistoric landscape transformation triggered by the settlement agglomeration at Maidanets'ke is proposed to have initiated the onset of local Chernozem formation.

Considering processes that would explain the burial of the Chalcolithic sites with mineral soil, aeolian addition of material might play a role. However, the mineral inventory indicates no aeolian addition from a different material source (Fig. 3c). Regional to local translocation of material by wind action is also improbable, taking into account the recorded similar pedo-stratigraphy of all Tryplian sites from the region (Kruts, 2012; Chapman et al., 2016). Instead, geophysical and geochemical data point to a very close relationship between the Chernozem and the subsoil (Figs. 6, 8). Thus, a process, explaining addition of subsoil to the surface is sought. Burrowing mammals contribute to vertical mixing of soil material (e.g. Paton et al., 1995). However, their activity would not produce the observed "quasi-linear age-depth relations" nor the crumb structure of Chernozem organic-mineral-soil-aggregates (e.g. Scharpenseel et al., 1986; Darwin, 1881; Lee, 1985; Kubiena, 1953). Surface casting- the accumulation of excremental aggregates- by anecic earthworms is, however, a process worth considering in detail. In the 19th century, Charles Darwin (Darwin, 1840; 1881) recognized that the surface casting process forms fertile topsoil that buries objects and layers of material too large to be ingested by the earthworms. Anecic earthworms usually have deep vertical burrows and feed on organic material at the surface (e.g. Bouché, 1977). They clean their burrow channels from material fallen in, mixing it in their intestines with the digestion products of fresh litter and cast it into subsoil cavities or on the soil surface. Earthworm surface castings observed at present day Maidanets'ke and Chernozem properties support the role of anecic earthworms in the soil formation process (Fig. 2a).

The Ah horizon is thinner above the archaeological remains. Since floor and daub layers are denser than the surrounding Loess, the smaller

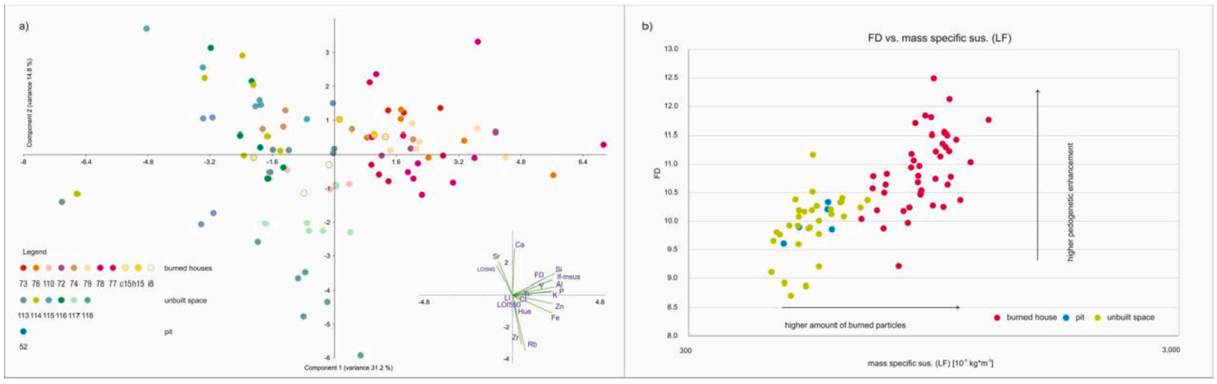

Fig. 8. Statistical comparisons of the investigated Ah horizons at Maidanets'ke, displaying the very close relationship between the Chernozem and its subsoil a) PCA based on correlation, b) plot of FD vs. low frequency susceptibility (Dearing, 1999).

Ah horizon thickness could reflect less suitable digging conditions to earthworms (e.g. Edwards and Lofty, 1977). Further, regularly observed differences of the burial depth of the archaeological record- e.g. the dipping of outer parts of the daub layers- could be explained by less restricted burrowing conditions for anecic earthworms along the outer rims of dense layers. The presence of thicker rBw horizons beneath dense archaeological layers or colluvial covers points towards the same direction: where burrowing is unimpeded, the rBw disappeared stepwise since it became incorporated into the evolving Chernozem Ah horizon (Fig. 7b). This could deliver an explanation for the widespread observed lack of Holocene precursor soils beneath Chernozems, while their later alteration e.g. into Cambisols or Luvisols is observed (e.g. Eckmeier et al., 2007; Dreibrodt et al., 2013).

The Chernozem horizon has a finer texture than the subsoil, which would mirror the preferred ingestion of finer particles by earthworms (e.g. Darwin, 1881; Evans, 1948; Landmaid, 1964). A Chernozem texture finer than subsoil is reported from other sites (e.g. Altermann et al., 2005). The sandier layers observed in c. 100 cm depth in our profiles could reflect local forms of "grit layers" (e.g. Darwin, 1881; Canti, 2003), indicating mean burrowing depth of anecic earthworms.

At Maidanets'ke, the unaltered Loess exposed a low frequency mass-specific magnetic susceptibility of 21.6 10^{-6} kg*m^{-3} (SD 3.4, n = 18). It experienced a pedogenetic enhancement of 66 % in the relict Bw horizons (35.9 10^{-6} kg*m^{-3}, SD 5.7, n = 19) and of about 143 % and 320 % in the Chernozem on unbuilt space (52.5 10^{-6} kg*m^{-3}, SD 7.2, n = 34) respectively above burned houses (90.9 10^{-6} kg*m^{-3}, SD 12.1, n = 47). The latter values might reflect the ingestion of fine magnetic particles from the archaeological record and the incorporation into their casts and thus into the growing Ah horizon partly (Fig. 8b). There is a significant pedogenetic enhancement over the archaeological record, too. This is paralleled by higher total phosphorus contents originating from the archaeological record and lower TOC:TN values in the evolving soil compared to the Chernozem on unbuilt space (Fig. 6). While these are often lacking during the analysis of Chernozem soil samples, bacterial consortia in earthworm intestines (e.g. Edwards and Bohlen, 1996; Doube and Brown, 1998) may contribute to the enrichment of magnetic particles, and thus explaining partly the so far not well understood pedogenetic magnetism of Chernozems (e.g. Maher and Thompson, 1995, 1999; Maher et al., 2003; Dearing et al., 1996; Jordanova, 2017).

The coexistence of tree (dominantly *Fraxinus*) and grass leaf lipid biomarkers within the Chernozem deserves a consideration (Fig. 4). While traditionally Chernozems are attributed to steppe conditions, according to palaeoecological findings at a rising number of mainly temperate humid Chernozem sites a soil genesis under forest has been concluded (e.g. Ehwald et al., 1999; Andreeva et al., 2011; Vysloužilova et al., 2014). Taking into account the anecic earthworm-casting hypothesis as outlined here (Fig. 7b), the "seemingly" forest pattern of the lipid biomarkers would result from the incorporation of rBw material into the earthworm casting process. The admixed grass lipids would reflect the fresh food of the earthworms gathered at the surface. The predominance of tree leaf lipids backs the model of incorporation of the rBw into the evolving Ah horizon. The interpretation of the sandy layer as a local form of "grit layer" would explain why few grass leaf lipids from the Löss below this sandy layer became incorporated into the Chernozem. Given the small size of many other bioremains (e.g. pollen, spores, phytoliths, charcoal particles) their incorporation into the evolving Chernozem could be explained likewise.

Summarizing, anecic-earthworm surface casting followed by a compaction of the loose casts delivers the best explanation for the genesis and properties of Chernozem at Maidanets'ke.

Understanding the relation between the impact of prehistoric agriculture on the landscape at Maidanets'ke and anecic earthworm activity needs a consideration of earthworm ecology. (Fig. 9)

Recent earthworm abundance increases in the order: modern agricultural fields (heavy machinery, chemicals) < deciduous forests ≪ grasslands ≪<≪ orchards/ pastures (Edwards and Bohlen, 1996; Evans, 1948; Satchell, 1967; 1983; Knollenberg et al., 1985). The earthworm forage available within deciduous woodlands is limited by leaf-fall in autumn. Grasslands and prehistoric agricultural plots established by the Chalcolithic settlers provided earthworms with food over the entire vegetation period, including dung known to stimulate earthworm abundance immensely (e.g. Satchell, 1967). The soil microclimate also affects the living conditions of earthworms; the amplitudes of summer temperatures and related water content of the soils are critical (e.g. Bouché, 1971, 1977). As these amplitudes became more pronounced in an opened landscape compared to a previous woodland, anecic earthworms were favored at the expense of epigeic or endogeic earthworms, near-surface-dwelling species, since the former escape disadvantageous seasonal topsoil conditions during summer and winter by digging into deeper layers. A predominance of anecic species in open landscapes has been observed in global surveys (Phillips et al., 2019). Irmler (1999) found the highest abundances of anecic species in open landscapes (agricultural fields, meadows) and negligible abundances below forests even in temperate landscapes as humid as northern Germany. Furthermore, the abundance of anecic species (i.e. *Lumbricus terrestris*) increased c. fivefold as a result of an 8 year period of organic farming compared to conventional farming (Irmler, 2010). Since the organic farming practice (minimal invasive plowing, few chemicals) is probable to reflect the preindustrial and prehistoric habitat conditions better, this makes a proliferation of anecic earthworm species by preindustrial farming probable. Considering the often-reported quasi-linear age depth gradients of Chernozems (Scharpenseel et al., 1986; Lisetskii et al., 2013, Fig. 7), we argue the predominant role of anecic earthworms on Chernozem solum formation, while endogeic species might be present as well. Due to their ecology (cleaning their vertical burrows permanently from material fallen in and putting it onto the soil surface in the form of

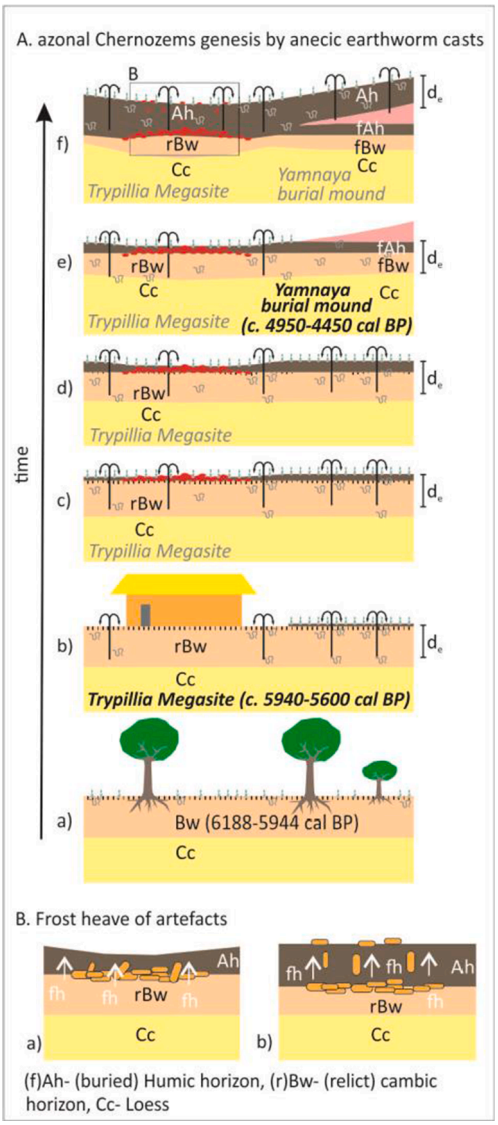

Fig. 9. Maidanets'ke soil formation. A: a) Forest steppe with a mixed earthworm population, b) Chalcolithic landscape opening creates microclimatic conditions favouring anecic earthworms; their abundance increases - surface casting and deeper soil mixing (d_e ~ 90–100 cm), c) Abandoned settlement, still open landscape; casting and mixing continues, d) casting layer grows, except where blocked by house floor, archaeological features 'sink', e) Yamnaya culture burial mound on top of "incipient-Chernozems" f) Continued worm casting covers Yamnaya burial mound and settlement. Note the faster sinking of the outer parts of the archaeological layers. B: Frost heave of archaeological artefacts by a) rotation and b) heave. d_e- depth of anecic earthworm digging, f_h- frost heave.

casts), anecic earthworms move soil particles permanently in slow rates upwards, whereas endogeic earthworms rather mix the solum horizontally (e.g. Bouché, 1971, 1977).

The simple model of the Ah horizon formation by anecic earthworm-surface-casting explains the observed pedo-stratigraphy, properties, and age-depth functions of SOM radiocarbon ages (Fig. 8b). A local mean burrowing depth of anecic earthworms is assumed. This would reflect a balance of soil depth sufficient to enable survival of anecic earthworms (summer drought, heat; winter frost) and the limits of energetic costs for digging by the earthworms. The former is controlled by local climate; the latter is a function of food availability. The sandy "grit layer" observed at a depth of c. 100 cm (Fig. 3a) could indicate this local depth at Maidanets'ke. Some processes of Ah horizon shortening (inwash of surface soil particles via macro pores, erosion) are neglected here. Surface related input of soil organic matter is considered to reflect mainly dead root biomass and its derivatives. For the sake of simplicity, the rates of the processes are assumed to be constant over time. Once the anecic surface casting process has started, the Ah horizon is growing in thickness at the surface. Since the process involves an incorporation of subsoil matter (earthworm burrows) it could be considered as a cycling between subsoil and topsoil and might not result in a substantial change in elevation. This is reflected in our record by the differences in the subsoil horizon preservation (rBw thicknesses) and the burial of the archaeological record, where the former implies a "consumption" of the relict subsoil horizon and the latter a "sinking" rather than a burial. Thus, the same mass of cast material that is added to the surface is subtracted from the subsoil, and consequently, the whole sequence is sinking ("subsidence") at the same rate as it is growing. The main root zone, which is contemporaneously adding SOM to the evolving surface horizon, is kept at the upper part of the evolving Ah horizon. At the point, when the Ah thickness equals the mean depth of anecic earthworm digging no further growth in Ah horizon thickness would result from ongoing surface casting since a recycling of the lower Ah horizon by the casting process starts. This would explain why Chernozems display regional limits in thickness and exceed seldom a thickness of 100–150 cm.

The described scenario would explain the record of Chernozem, the relict subsoil (rBw) and the burial of the archaeological record at Maidanets'ke. The asymptotical form of the age-depth gradient in the thick undisturbed profile 117 would reflect a stepwise increased amount of aged lower Chernozem Ah material to the casting process, fallen into the earthworm diggings and "re-added" to the surface by fresh casts.

The integration of pedostratigraphy and SOM radiocarbon ages at Maidanets'ke questions the traditional interpretation of age-depth gradients resulting from Chernozem growth rates (e.g. Scharpenseel et al., 1986; Lisetskii et al., 2013) and highlight the need for anchoring Chernozem ages by independent age information (e.g. archaeological layers), as might exist in many Chernozems.

Summarizing the results from Maidanets'ke, we argue that the distinct landscape transformation by agricultural activities of prehistoric communities facilitated the proliferation of anecic earthworms, which started the surface casting process and Chernozem formation (Fig. 4). After Maidanets'ke's abandonment, the regional climate and the felted root system of steppe grasses (e.g. Walter and Breckle, 1994) impeded a fast reforestation. Subsequent phases of prehistoric agropastoralism, archaeologically record in the region (e.g. Dreibrodt et al., 2020), maintained favorable living conditions for anecic earthworms in the Ukrainian forest-steppe, and extended regional Chernozem formation towards the northern forest border, until the onset of adverse conditions in modern agroecosystems.

To explain the occurrence of ceramic sherds and pieces of daub within the soil and at its present surface the implementation of another process into the described conceptual model is necessary. Besides some artefacts that might be unearthed by burrowing mammals, the addition of the long-known process of frost heaving (e.g. Washburn, 1979) to our model of Chernozem genesis explains the existence of finds within the Chernozem A-horizon above archaeological findings. Although more attention to these processes was paid in periglacial environments, surface soils are exposed to frost in temperate regions of the northern hemisphere today (e.g. Hartge, 1978; Selezneva et al., 2008). In the region around Maidanets'ke, at least three months exhibit temperatures below −2 °C (www.climate-data.org, 2020). Thus, single finds will become affected by frost heaving. Single finds (e.g. pottery sherds) will appear in the soil above the buried archaeological record if the rate of frost heaving of artefacts is equal or higher than the earthworm-casting rate. Additionally, the frost heave process might stay in action during interruptions of the earthworm casting process (e.g., phases of reforestation, intensive modern agricultural practices). In fact, the traditional archaeological field method of surface surveys frequently takes

advantage of the result of the outlined process in many European landscapes.

5.2. Larger scale implications

Chernozem occurrences in temperate humid Europe (Fig. 1a) (e.g. Soil Atlas of Europe, 2015; Eckmeier et al., 2007), where land would naturally be covered by forest-steppe or woodlands (Bohn et al., 2004) have a conspicuous distribution pattern, placing the results from the Ukrainian forest-steppe ecotone into a larger context. The temperate humid European Chernozems developed predominantly on Loess along the eastern pathway of the Neolithic transition of Europe: in Bulgaria, along the Danube, in the Pannonian Basin and in northern Central Europe (e.g. Gronenborn and Petrasch, 2010; Vander Linden and Silva, 2018; Banffy et al., 2019). The anecic earthworm surface-casting hypothesis outlined at the example of Maidanets'ke explains those Chernozem occurrences in temperate humid Europe. Prehistoric farmers locally facilitated the presence of anecic earthworms and surface casting, leading to lower species diversity of earthworms paralleled with high biomass (Phillips et al., 2019; Rutgers et al., 2016). The local openings would explain the patchy distribution of many temperate humid Chernozems and their invisibility in regional vegetation records displayed by pollen profiles, too (e.g. Müller, 1953; Litt, 1994; Ehwald et al., 1999). As a consequence of the varied timing of extensive prehistorical agricultural impacts and its duration, Chernozem ages differ from c. 6950 cal BP in southern Bulgaria (Fol et al., 1988) to c. 5950 cal BP in Maidanets'ke, and younger (c. 5550–1850 cal BP) in northern central Europe (e.g. Eckmeier et al., 2007). Pyrogenic carbon, whether of anthropogenic origin or not, preserved in German Chernozem (e.g. Schmidt et al., 2002) became incorporated into the soil via the surface casting process of anecic earthworms. Neolithic sites on Loess without Chernozem (Lorz and Saile, 2011) indicate woodland openings that were too short in time and/or too small in area to establish enduring favorable conditions for anecic earthworms. Consequently, temperate humid Chernozems are present in regions with longer lasting, repeatedly settled prehistorical agricultural landscapes in central and southeast Europe (Banffy et al., 2019). Insular Chernozem occurrences apart from the outlined migration pathways along the European river valleys, as on Loess sites in Poland (e.g. Labaz et al., 2018; Kabała et al., 2019) are explainable as well. The recorded intensive land use phase of the Funnel Beaker culture at the Polish site might have created a soil environment proliferating anecic earthworms and thus resulting in a further development of an early Holocene relict Chernozem. Later on, the Chernozem has become preserved only where buried deep enough by a grave mound, whereas it is gone in the surroundings after reforestation led to adverse habitat conditions for anecic earthworms and the transformation of the Chernozem into forest soil (Luvisol). We argue that the hypothesis of anecic earthworm casting proliferated by pre-industrial agriculture is able to explain the varying and partly contradictory records on Chernozems across Europe. Whereas the temperate humid Chernozems formed in agriculturally opened landscape, favoring the prosperity of anecic earthworms at the expense of epigeic and endogeic species as a result of land use, the natural conditions limit the latter groups of earthworms in climatic steppe and thus may explain the climatic steppe Chernozem as well. Dokuchaev (1883) and his followers might have overseen the maintenance of anecic earthworms for Chernozem formation since they carried out their pioneer work mainly in summer seasons, when the earthworms are inactive. Additionally, the comparatively slow surface casting rates might have led to an underestimation of their long-term consequences (see discussion Darwin- Mr. Fish; Darwin, 1869).

6. Conclusions

The outlined surface-casting hypothesis developed at Maidanets'ke, central Ukraine, explains the record of European Chernozems. The related processes add another strand of research on soil carbon sequestration considering the dynamics of carbon stocks of Chernozems and their future management. The observed prehistoric human-soil interrelationships add further points to early anthropogenic impact on landscapes. Since the Neolithic transition was a decisive period in European human history and the outlined hypothesis generates new research questions, for example: Should temperate humid Chernozem formation be considered in the "Anthropocene discussion" (e.g. Zalasiewicz et al., 2008; Lane, 2015) or: Should earthworms be regarded as part of the "Neolithic Package"? Considering the importance of earthworms in the development of the fertile Chernozem soils, this points also to the future of modern agricultural methods and their environmental consequences.

Declaration of Competing Interest

The authors declare that they have no known competing financial interests or personal relationships that could have appeared to influence the work reported in this paper.

Acknowledgements

This work was supported by the Deutsche Forschungsgemeinschaft (DFG), Collaborative Research Centre 1266 'Scales of Transformation' [project number 2901391021]. We are grateful to the landowners that enabled the fieldwork and V. Chabanuk (State Historical and Cultural Reserve Trypillia Culture, Legedzyne) for excellent support in logistical and scientific matters. We are grateful to two unknown reviewers. Their comments on an earlier version of the manuscript helped to improve the quality of the work.

References

Boden, A.G., 2005. Bodenkundliche Kartieranleitung. Schweizerbart'sche Verlagsbuchhandlung, Stuttgart.
Altermann, M., Rinklebe, J., Merbach, I., Körschens, M., Langer, U., Hofmann, B., 2005. Chernozem—Soil of the Year 2005. J. Plant Nutr. Soil Sci. 168, 725–740.
Andreeva, D.B., Leiber, K., Glaser, B., Hambach, U., Erbajeva, M., Chimitdorgieva, G.D., Tashak, V., Zech, W., 2011. Genesis and properties of black soils in Buryatia, southeastern Siberia, Russia. Russia, *Quaternary International* 243, 313–326.
Atlas of Soils of the Ukrainian Socialistic Soviet Republic, 1979. (in Russian), Harvest. Kiew.
Bánffy, E., Hoffmann, K.P., v. Rummel, P., 2019. *Spuren des Menschen*, WBG Darmstadt.
Bohn, U., Gollub, G., Hettwer, C., Neuhäuslová, Z., Raus, T., Schlüter, H., Weber, H., 2004. Map of the natural vegetation of Europe. BfN, Münster.
Bond, G., Kromer, B., Beer, J., Muscheler, R., Evans, M.N., Showers, W., Hoffmann, S., Lotti-Bond, R., Hajdas, I., Bonani, G., 2001. Persistant solar influence on north atlantic climate during the holocene. Science 294, 2130–2136.
Bouché, M.B., 1971. In: *La Vie dans les Sols, Aspects Nouveaux, Études Experimentales* (ed. Pesson, P.) Gauthier-Villars, Paris, pp. 187-209.
Bouché, M.B., 1977. In: *Soil Organisms as Components of Ecosystems* (eds. Lohm, U., Persson, T.), Ecol. Bull. 25, Stockholm, pp. 122-132.
Brindley, G.W., Brown, G., 1980. Crystal Structures of Clay Minerals and their X-Ray Identification. Mineralogical Society, London.
Bronk Ramsey, C., Lee, S., 2013. Recent and planned developments of the program OxCal. *Radiocarbon* **55,** 3–4 (2013).
Canti, M.G., 2003. Earthworm activity and archaeological stratigraphy: a review of products and processes. J. Archaeol. Sci. 30, 135–148.
Chapman J, Gaydarska B, Hale D., 2016. In: *Trypillia Mega-Sites and European Prehistory 4100–3400* (eds Müller, J., Rassmann, K., Videiko, M.), Routledge, London, pp. 117-132.
Dal Corso, M., Hamer, W., Hofmann, R., Ohlrau, R., Shatilo, L., Knitter, D., Dreibrodt, S., Saggau, P., Duttmann, R., Feeser, I., Knapp, H., Benecke, N., Videiko, M., Müller, J., Kirleis, W., 2019. Modelling landscape transformation at the Chalcolithic Tripolye mega-site of Maidanetske (Ukraine): Wood demand and availability. The Holocene 29 (10), 1622–1636.
Darwin, C., 1840. On the formation of mould. Transactions of the Geological Society of London 5, 505–509.
Darwin, C., 1869. *Gardeners' Chronicle and Agricultural Gazette* (1869): 530, https://www.darwinproject.ac.uk/letter/DCP-LETT-6738.xml.
Darwin, C., 1881. *The Formation of Vegetable Mould through the Action of Worms, with Observation of their habits*, Murray, London.
Dearing, J., 1999. *Environmental Magnetic Susceptibility: Using the Bartington MS2 System*. 2nd ed., Bartington Instruments Ltd.
Dearing, J.A., Dann, R.J.L., Hay, K., Lees, J.A., Loveland, P.J., Maher, B.A., O'Grady, K., 1996. Frequency-dependent susceptibility measurements of environmental material. Geophys. J. Int. 127, 228–240.

Dreibrodt, S., Jarecki, H., Lubos, C., Khamnueva, S.V., Klamm, M., Bork, H.-R., 2013. Holocene soil formation and soil erosion at a slope beneath the Neolithic earthwork Salzmünde (Saxony-Anhalt, Germany). Catena 107, 1–14.
Dreibrodt, S., Furholt, M., Hofmann, R., Hinz, M., Cheben, I., 2017. P-Ed-XRF-Geochemical Signatures of a 7300 Year Old Linear Band Pottery House Ditch Fill at Vráble-Ve'lké Lehemby, Slovakia - House Inhabitation and Post-Depositional Processes. Quat. Int. 438, 131–143.
Dreibrodt, S., Hofmann, R., Sipos, G., Schwark, L., Videiko, M., Shatilo, L., Martini, S., Saggau, P., Bork, H.-R., Kirleis, W., Duttamnn, R., Müller, J., 2020. Holocene soil erosion in Eastern Europe-land use and/or climate controlled? The example of a catchment at the Giant Chalcolithic settlement at Maidanetske, central Ukraine. *Geomorphology* 367. https://doi.org/10.1016/j.geomorph.2020.107302.
Driessen, P., Deckers, J., Spaargargen, O., Nachtergaele, F., 2001. Lecture Notes on the Major Soils of the World. FAO, Rome.
Dokuchaev, V.V., 1883. *Russkij Cernozem: Otchet Imperatorskomu volnomu yekonomicheskomu obschestvu,* Sankt-Peterburg.
Eckmeier, E., Gerlach, R., Gehrt, E., Schmidt, M.W.I., 2007. Pedogenesis of Chernozems in Central Europe — A review. Geoderma 139, 288–299.
Edwards, C.A., Bohlen, P.J., 1996. Biology and Ecology of Earthworms. Chapman & Hall, London.
Edwards, C.A., Lofty, J.R., 1977. Biology of Earthworms. Chapman & Hall, London.
Ehwald, E., Jäger, K.-D., Lange, E., 1999. Das Problem Wald-Offenland im zirkumhercynen Trockengebiet vor der neolithischen Besiedlung sowie die Entstehung der zirkumhercynen Schwarzerden. In: Rolle, R., Andraschko, F.M. (Eds.), Frühe Nutzung pflanzlicher Ressourcen. Internationales Symposium Duderstadt, Lit, Hamburg, pp. 12–34.
Eswaran, H., Almaraz, R., van den Berg, E., Reich, P., 1997. An assessment of the soil resources of Africa in relation to productivity. Geoderma 77, 1–18.
Evans, A.C., 1948. Studies on the relationships between earthworms and soil fertility. II. Some effects of earthworms on soil structure. Ann. Appl. Biol. 35, 1–13.
FAO, 2014. *World reference base for soil resources* (FAO, Rome, 2014).
Filzmoser, P., Hron, K., Reimann, C., 2009. Principle component analysis for compositional data with outliers. Environmetrics 20, 621–632.
Fol, A., Katrinčarow, R., Lichardus, J., 1988. Die bulgarisch-deutschen Ausgrabungen in Varna. Moderne Galerie des Saarland Museums, Saarbrücken.
Gehrt, E., Geschwinde, M., Schmidt, M.W.I., 2002. Neolithikum, Feuer und Tschernosem – oder: was haben die Linearbandkeramiker mit der Schwarzerde zu tun? Archäologisches Korrespondenzblatt 32, 21–30.
Gerasimenko, N., 1997. In: *Third Millennium BC Climate Collapse and Old World Change* (eds Dalfes, H.N., Kukla, G., Weiss, H.), Springer, Berlin, pp. 371-399.
Gronenborn, D., Petrasch, J., 2010. Die Neolithisierung Mitteleuropas. Schnell + Steiner, Regensburg.
Hartge, K.H., 1978. Einführung in die Bodenphysik. Enke Verlag, Stuttgart.
Harper, T.K., 2019. Demography and climate in Late Eneolithic Ukraine, Moldova, and Romania: Multiproxy evidence and pollen-based regional corroboration. J. Archaeol. Sci. Rep. 23, 973–982.
Hofmann, R., Müller, J., Shatilo, L., Videiko, M., Ohlrau, R., Rud, V., Burdo, N., Dal Corso, M., Dreibrodt, S., Kirleis, W., 2019, Governing Tripolye: Integrative architecture in Tripolye settlements. *PLoSONE* **14**(9): e0222243. https://doi.org/10.13 71/journal.pone.0222243.
Irmler, U., 1999. Die standortüblichen bedingungen der regenwürmer (Lumbricidae) in schleswig-holstein. Faunistisch-Ökologische Mitteilungen 7, 509–518.
Irmler, U., 2020. Changes in earthworm populations during conversion from conventional to organic farming. Agric. Ecosyst. Environ. 135, 194–198.
Ivanova, S.I., 2016. In: *Interactions, Changings and Meanings* (eds. Terna, S., Govedarica, B.), University of high Anthropological School, Kishinev, pp. 273-291.
Jordanova, N., 2017. Soil Magnetism. Academic Press, Amsterdam.
Kabała, C., Przybył, A., Krupski, M., Łabaz, B., Waroszewski, J., 2019. Origin, age and transformation of Chernozems in northern Central Europe-New data from Neolithic earthen barrows in SW Poland. Catena 180, 83–102.
Kirleis, W., Dreibrodt, S., 2017. The Natural Background: Forest, Forest Steppe or Steppe Environment. In: Müller, J., Rassmann, K., Videiko, M. (Eds.), Trypillia-Megasites and European Prehistory 4100–3400 BCE. Maney Publishing, London/New York, pp. 171–180.
Knollenberg, W.G., Merrit, R.W., Lawson, D.L., 1985. Consumption of leaf litter by *Lumbricus terrestris* (Oligochaeta) in a Michigan woodland floodplain. Am. Midland Naturalist 113, 1–6.
Kremenetski, C.V., 1995. Holocene vegetation and climate history of southwestern Ukraine. Rev. Palaeobot. Palynol. 85, 289–301.
Kruts V., 2012. in: *The Tripolye Culture Giant-Settlements in Ukraine. Formation, Development and Decline* (eds Menotti, F., Korvin-Piotrovskiy, A.G.), Oxbow Books, Oxford, pp. 70-78.
Kubiena, W.L., 1953. The Soils of Europe. Murby, London.
Łabaz, B., Musztyfaga, E., Waroszewski, J., Bogacz, A., Jezierski, P., Kabała, C., 2018. Landscape-related transformation and differentiation of Chernozems-Catenary approach in the Silesian Lowland, SW Poland. *Catena* 161, 63–76.
Landmaid, K.K., 1964. Some effects of earthworm invasion in virgin Podsols. Can. J. Soi. Sci. 44, 34–37.
Lane, P.J., 2015. Archaeology in the age of the Anthropocene: A critical assessment of its scope and societal contributions. J. Field Archaeol. 40, 5. https://doi.org/10.1179/2042458215Y.0000000022.
Lee, K.E., 1985. Earthworms: Their Ecology and Relationships with Soils and Land Use. Academic Press, Sydney.
Lisetskii, F.N., Goleusov, P.V., Chepelev, O.A., 2013. The development of chernozems on the dniester-prut interfluve in the holocene. Eurasian Soil Science 46, 491–504.
Litt, T., 1994. Paläoökologie, Paläobotanik und Stratigraphie des Jungquartärs im nordmitteleuropäischen Tiefland, *Dissertationes Botanicae* **227**.
Lorz, C., Saile, T., 2011. Anthropogenic pedogenesis of Chernozems in Germany? - A critical review. Quat. Int. 243, 273–279.
Lubos, C., Dreibrodt, S., Bahr, A., 2016. Analysing spatio-temporal patterns of archaeological soils and sediments by comparing pXRF and different ICP-OES extraction methods. J. Archaeolog. Sci.: Rep. 9, 44–53.
Machow, G., 1930. Soils of Ukraine, Kiew.
Maher, B.A., Thompson, R., 1995. Paleorainfall reconstructions from pedogenic magnetic susceptibility variations in the Chinese loess and paleosols. Quat. Res. 44, 383–391.
Maher, B.A, Thompson, R., 1999. In: *Quaternary Climates, Environments and Magnetism* (eds Maher, B., Thompson, R.), Cambridge University Press, Cambridge, pp. 117-132.
Maher, B.A., Yu, H.M., Roberts, H.M., Wintle, A.G., 2003. Holocene loess accumulation and soil development at the western edge of the Chinese Loess Plateau: implications for magnetic proxies of paleorainfall. Quat. Sci. Rev. 22, 445–451.
Martini, S.J., Athanassov, B., Frangipane, M., Rassmann, K., Stockhammer, P.W., Dreibrodt, S., 2019. A budgeting approach for estimating matter fluxes in archaeosediments, a new method to infer site formation and settlement activity: Examples from a transect of multi-layered Bronze Age settlement mounds. J. Archaeolog. Sci.: Rep. 26, 101916.
Matviishyna, Z.M., Doroshkevych, S.P., 2016. Reconstruction of natural Atlantic stage conditions based on the paleosoil research of Trypillia settlement. Ukrainskii Geographic Journal 2, 19–25.
Mayewski, P.A., Meeker, L.D., Twickler, M.S., Whitlow, S., Yang, Q., Lyons, W.B., Prentice, M., 1997. Major features and forcing of high-latitude northern hemisphere atmospheric circulation using a 110,000-year-long glachiochemical series. J. Geophys. Res. 102, 26345–26366.
Müller, H., 1953. Zur spät- und nacheiszeitlichen Vegetationsgeschichte des Mitteldeutschen Trockengebietes. Nova Acta Leopoldina N.F. 16/110.
Müller, J., Hofmann, R., Kirleis, W., Dreibrodt, S., Ohlrau, R., Brandtstätter, L., Dal Corso, M., Out, W., Rassmann, K., Burdo, N., Videiko, M., 2017. *Maidanetske 2013. New excavations at a Tripyllia mega-site. Studien zur Archäologie in Ostmitteleuropa* **16**, Habelt, Bonn.
Müller, J., Rassmann, K., Videiko, M., 2016. *Tripyllia Mega-Sites and European Prehistory 4100-3400 BCE. Themes in Contemporary Archaeology* **2**, Routledge, London.
Novenko, E.Y., Tsyganov, A.N., Rudenko, O.V., Volkova, E.V., Zuyganova, I.S., Babeshko, K.V., Olchev, A.V., Losbenev, N.I., Payne, R., Mazei, Y.A., 2016. Mid-and late-Holocene vegetation history, climate and human impact in the forest-steppe ecotone of European Russia: New data and a regional synthesis. Biodivers. Conserv. 25, 2453–2472.
Ohlrau, R., 2020. Maidanets'ke. Development and decline of a Trypillian mega-site in Central Ukraine. Sidestone Press, Leiden.
Paton, T.R., Humpreys, G.S., Mitchell, P.B., 1995. Soils. UCL Press, London, A new global perspective.
Phillips, H.R.P., et al., 2019. Global distribution of earthworm diversity. Science 366, 480–485.
Pickartz, N., Hofmann, R., Dreibrodt, S., Rassmann, K., Shatilo, L., Ohlrau, R., Wilken, D., Rabbel, W., 2019. Deciphering archeological contexts from the magnetic map: Determination of daub distribution and mass of Chalcolithic house remains. The Holocene 29 (10), 1637–1652.
Rabenhorst, M.C., Schmehling, A., Thompson, J.A., Hirmas, D.R., Graham, R.C., Rossi, A. M., 2014. Reliability of Soil Color Standards. Soil Sci. Soc. Am. J. 79, 193–199.
Rutgers, M., et al., 2016. Mapping earthworm communities in Europe. Appl. Soil Ecol. 97, 98–111.
Sanmartín, P., Chorro, E., Vázquez-Nion, D., Miguel Martínez-Verdú, F., Prieto, B., 2014. Conversion of a Digital Camera into a Non-Contact Colorimeter for Use in Stone Cultural Heritage: The Application Case to Spanish Granites. Measurement 56, 194–202.
Satchell, J.E., 1967. In: *Soil Biology* (eds Burgess, A., Raw, F.), Academic Press, London, pp. 259-322.
Satchell, J.E., 1983. In: *Earthworm Ecology: From Darwin to Vermiculture* (ed Satchell, J. E.), Chapman & Hall, London, pp. 161-170.
Scharpenseel, H.W., Tsutsuki, K., Becker-Heidmann, P., Freytag, J., 1986. Untersuchungen zur Kohlenstoffdynamik und Bioturbation von Mollisolen. Z. Pflanzenernaehr. Bodenk. 149, 582–597.
Schmidt, M.W.I., Skjemstad, J.O., Jäger, C., 2002. Carbon isotope geochemistry and nanomorphology of soil black carbon: Black chernozemic soils in central Europe originate from ancient biomass burning. Global Biogeochem. Cycles 16 (art, no.1123).
Singh, M., Ram, N., 1996. Effect of soil enrichment with zinc on crop yields and its replenishment in Mollisols of northern India. Agrochimica 40, 19–24.
Seiler, M., Grootes, P., Haarsaker, J., Lélu, S., Rzadeczka-Juga, I., Stene, S., Svarva, H., Thun, T., Værnes, E., Nadeau, M.-J., 2019. Status report of the Trondheim Radiocarbon Laboratory. Radiocarbon 61 (6), 1963–1972.
Selezneva, O.I., Jiang, Y.J., Larson, G., Puzin, T., 2008. Long Term Pavement Performance- Computed Parameter: Frost Penetration, FHWA-HRT-08-057. U.S, Department for Transportation, Georgetown Pike.
Shmaglij, N.M., Videiko, M.Y., 2001. Maidanetskoe: tripolskii protogorod. Stratum Plus 2, 44–140.
Soil Atlas of Europe, 2005. European Soil Bureau Network European Commission. Office for Official Publications of the European Communities, Luxembourg.
Tanov, Y., 1956. Soil Map of Bulgaria 1:200000, Sofia.
Vander Linden, M., Silva, F., 2018. Comparing and modeling the spread of early farming across Europe. Past Global Changes Magazine 26 (1), 28–29.

Vysloužilova, B., Danková, L., Ertlen, D., Novák, J., Schwartz, D., Šefrna, L., Delhon, C., Berger, J.-F., 2014. Vegetation history of chernozems in the Czech Republic. Veget Hist Archaeobot 23, 97–108.
Viscarra Rossel, R.A., Minasny, B., Roudier, P., McBratney, A.B., 2006. Colour Space Models for Soil Science. Geoderma 133, 320–337.
Walter, H., Breckle, S.-W., 1994. Ökologie der Erde, vol. 3. Fischer, Stuttgart.
Washburn, A.L., 1979. Geocryology: A Survey of Periglacial Processes and Environments. Edward Arnold, London.
Weninger, B., Clare, L., Rohling, E.J., Bar-Yosef, O., Böhner, U., Budja, M., Bundschuh, M., Feurdean, A., Gebel., H.-G., Jöris, O., Linstädter, J., Mayewski, P., Mühlenbruch, T., Reingruber, A., Rollefson, G., Schyle, D., Thissen, L., Todorova, H., Zielhofer, C., 2009. The Impact of Rapid Climate Change on prehistoric societies during the Holocene in the Eastern Mediterranean, *Documenta Praehistorica* **XXXVI**, 551-583.
www.climate-data .org, 2020- https://de.climate-data.org/europa/ukraine/oblast-tscherkassy/uman-25308/#climate-table.
Zalasiewicz, J., Williams, M., Smith, A., Barry, T.L., Coe, A.L., Bown, P.R., Brenchley, P., Cantrill, D., Gale, A., Gibbard, P., Gregory, F.G., Hounslow, M.W., Kerr, A.C., Pearson, P., Knox, R., Powell, J., Waters, C., Marshall, J., Oates, M., Rawson, P., Stone, P., 2008. Are we now living in the Anthropocene? GSA Today 18 (2), 4–8.